

Lawrence Berkeley National Laboratory

Lawrence Berkeley National Laboratory

Title

Electrical properties of inalp native oxides for metal-oxide-semiconductor device applications

Permalink

<https://escholarship.org/uc/item/30p742jd>

Authors

Cao, Y.
Zhang, J.
Li, X.
[et al.](#)

Publication Date

2004-09-01

Electrical properties of InAlP native oxides for metal-oxide-semiconductor device applications

Y. Cao,^{a)} J. Zhang, X. Li, T. H. Kosel, P. Fay, and D. C. Hall^{b)}

*Department of Electrical Engineering, University of Notre Dame, Notre Dame, Indiana
46556-5637*

X. Zhang and R. D. Dupuis

*School of Electrical and Computer Engineering, Georgia Institute of Technology, Atlanta,
Georgia 30332-0250*

J. B. Jasinski and Z. Liliental-Weber

Lawrence Berkeley National Laboratory, 1 Cyclotron Road, Berkeley CA 94720

Data are presented on the insulating properties and capacitance-voltage (CV) characteristics of metal-oxide-semiconductor (MOS) device-thickness (below ~100 nm) native oxides formed by wet thermal oxidation of thin InAlP epilayers lattice matched to GaAs. Low leakage current densities of $J=1.4 \times 10^{-9}$ A/cm² and $J=8.7 \times 10^{-11}$ A/cm² are observed at an applied field of 1 MV/cm for MOS capacitors fabricated with 17 nm and 48 nm oxides, respectively. TEM images show that the In-rich interfacial particles which exist in 110 nm oxides are absent in 17 nm oxide films. Quasi-static capacitance-voltage measurements of MOS capacitors fabricated on both *n*-type and *p*-type GaAs show that the InAlP oxide-GaAs interface is sufficiently free of traps to

support inversion, indicating an unpinned Fermi level. These data suggest that InAlP native oxides may be a viable insulator for GaAs MOS device applications.

Due to the wide array of high electron mobility alloys of varying bandgaps that can be epitaxially grown on its surface, GaAs remains the most widely used semiconductor for high-speed electronic applications. While Schottky gates are commonly used in high-speed GaAs transistors, the restricted forward bias (a few tenths of a volt) that can be applied without excessive gate leakage currents limits their power handling capability. The electrical characteristics of native oxides of GaAs are far inferior to those of SiO₂ on Si, and an alternative insulator has long been pursued^{1,2} to enable the preferred metal-insulator-semiconductor gate structure. Many deposited insulator/GaAs structures have been investigated, although only a few have yielded promising results.³⁻⁶ Native oxide films on GaAs can offer advantages of processing convenience and low cost. Wet thermal oxides of AlGaAs⁷ have been studied but found to suffer from midgap traps caused by residual interfacial As.⁸ These traps lead to increased interface recombination velocity^{9,10} and high leakage currents.¹¹ However, the wet thermal oxides of *As-free* In_{0.485}Al_{0.515}P (lattice matched to GaAs) have been found to possess excellent insulating^{12,13} and interfacial properties^{13,14} and may provide a viable native oxide for III-V MOS devices.

In this letter, we report on the electrical properties and microstructure of InAlP native oxides scaled to reduced thicknesses more suitable for MOS device applications than the 110 nm oxides reported previously.^{13,14} Current-voltage measurements on MOS capacitors fabricated with oxides formed from thin InAlP epilayers show very low leakage current densities while capacitance-voltage (C-V) measurements indicate that the thin

oxides support inversion. Transmission electron microscopy (TEM) images elucidate the microstructure of the InAlP native oxide of different thicknesses.

Samples are grown by metalorganic chemical vapor deposition (MOCVD). *N*-type heterostructures grown on Si-doped ($2 \times 10^{18} \text{ cm}^{-3}$) GaAs substrates consist of 500 nm of Si-doped ($\sim 10^{16} \text{ cm}^{-3}$) GaAs, an undoped $\text{In}_{0.485}\text{Al}_{0.515}\text{P}$ layer with one of three different thicknesses (63, 31 or 15 nm) and a 50 nm thick undoped GaAs cap layer. The *p*-type heterostructures are grown on semi-insulating GaAs substrates, and consist of 1000 nm and 500 nm C-doped GaAs layers ($2 \times 10^{18} \text{ cm}^{-3}$ and $1 \times 10^{17} \text{ cm}^{-3}$, respectively), an undoped $\text{In}_{0.485}\text{Al}_{0.515}\text{P}$ layer (63 nm, 31 nm or 15 nm), and a 50 nm undoped GaAs cap layer.

The GaAs cap layers are removed by a 4:1 citric acid: 30% H_2O_2 selective etch before samples are thermally oxidized at 500 °C from the surface in a 2 in. diameter quartz tube furnace with 0.68 l/min of UHP N_2 bubbled through 95 °C H_2O . The 63, 31 and 15 nm InAlP layers are fully oxidized and expand upon oxidation (for 65, 30 and 15 minutes, respectively) to corresponding oxide thicknesses (obtained from TEM images) of 110 ± 1.6 , 48 ± 1.7 and 17 ± 1.1 nm, respectively. Variable-angle spectroscopic ellipsometry (VASE) measurements show that the InAlP oxide has a real refractive index of ~ 1.58 for the wavelength range from 600-1700 nm and negligible absorption (imaginary index $k \leq 10^{-3}$) with an onset of absorption below 600 nm indicating a bandgap for the oxide (from a Tauc plot¹⁵) of ≥ 4.0 eV.¹⁶

Metal-oxide-semiconductor (MOS) structures are fabricated by the evaporation of Cr/Au gate electrodes onto the oxide surface. Current-voltage (I-V) measurements are carried out using an Agilent 4156C semiconductor parameter analyzer. Quasi-static and high-frequency (100 kHz) capacitance-voltage (C-V) measurements are performed using a Keithley model 82 C-V measurement system. All measurements are done at room temperature in a shielded probe station. All capacitors have a contact area of $240\ \mu\text{m} \times 240\ \mu\text{m}$ ($5.8 \times 10^{-4}\ \text{cm}^2$). TEM cross-sectional specimens were prepared by a standard methods of mechanical pre-thinning (with dimple grinding or wedge polishing) followed by 2 kV Ar-ion milling.

Figure 1 shows leakage current density versus electric field for MOS capacitors fabricated with (a) 17 nm and (b) 48 nm oxide films on *n*-type GaAs. The jaggedness appearing in (b) results from the 10 fA resolution of the measurement instrumentation. The electric field is obtained by dividing the applied voltage by the measured oxide thickness. At a field of 1 MV/cm, the measured leakage current densities are $1.4 \times 10^{-9}\ \text{A/cm}^2$ for the 17 nm oxide and $8.7 \times 10^{-11}\ \text{A/cm}^2$ for the 48 nm oxide. Breakdown fields for all InAlP native oxides in this letter are in the 3-6 MV/cm range. Table I lists a comparison of these leakage current density and breakdown field results with other native and deposited oxides on GaAs. At the same field strength, the 48 nm InAlP oxide of Fig 1 (b) exhibits more than one order of magnitude less leakage than the 64 nm $\text{Gd}_{0.31}\text{Ga}_{0.1}\text{O}_{0.59}/\text{Ga}_2\text{O}_3$ dielectric stack of Ref. [6]. Compared to other candidate

insulator/GaAs structures, InAlP native oxides clearly possess the excellent insulating properties needed for MOS device applications.

As shown in the bright-field TEM images of Fig. 2, dark particles exist near the oxide/GaAs interface in the 110 nm oxide of Fig. 2 (a), while no dark interfacial particles appear in the 17 nm oxide of Fig. 2 (b). Fig. 2 (b) is representative of the entire observable area for this and a second wedge-polished cross section specimen, with the absence of particles also confirmed for plan-view specimens (not shown) in which possible loss of particles due to ion milling and electron beam interactions is suppressed by the fact that they are protected from the vacuum by the substrate and overlying oxide film. The interfacial particles in Fig. 2 (a) are believed to be indium rich based on Z-contrast TEM images¹⁶ (not shown) and Auger depth profiling.¹⁷ The size of the particles increases with the progressive consumption of the InAlP epilayer during oxidation.¹⁶ We hypothesize that In, the heaviest element in the structure, outdiffuses more slowly than the other alloy constituents and hence accumulates near the interface during oxide growth, forming In-rich particles.

Figure 3 shows 100 kHz high-frequency (CH) and quasi-static (CQ) capacitance-voltage measurements for the 17 nm oxides on both *n*-type and *p*-type GaAs under standard microscope illumination as is required for wide bandgap semiconductors due to the low thermal generation rate of electron-hole pairs.¹⁸ The clear existence of three operational regimes – accumulation, depletion and inversion – of these MOS structures for both *n*- and *p*-type samples indicates that the Fermi level is unpinned.

Thicker oxides (48 nm and 110 nm) on both types of GaAs also show similar unpinned behavior (not shown). The frequency dispersion (offset between CQ and CH curves in accumulation) seen in Fig. 3 is commonly observed^{2,18,19} in III-V MOS structures. While possibly attributable to a low resistivity interfacial region of the oxide which reduces the effective oxide thickness and thus increases the apparent capacitance at low measurement frequencies (Maxwell-Wagner effect¹⁸), it is in general not well understood. Using bias-dependent swept-frequency impedance spectroscopy, a total interface state density of $8 \times 10^{11} \text{ cm}^{-2}$ has previously been found for the 110 nm oxide on n-type GaAs.¹⁴ The absence of particles in the interfacial region of the 17 nm oxide shown in Fig. 2 (b) may lead to a still lower interface state density for thinner InAlP oxide films.

In summary, with their excellent insulating properties and unpinned Fermi level, the native oxides of InAlP show promise for the gate dielectric in GaAs MOS device applications. Interfacial particles observed for thicker InAlP oxide films are not present in the thinner 17 nm oxide films, and leakage current densities are lower at equivalent field strength than the best reported results for comparable deposited oxide films. Wet thermal growth of InAlP native oxide films potentially offers a simpler, lower cost manufacturing technology for GaAs MOS devices.

Acknowledgements

The authors would like to acknowledge Dr. Gregory L. Snider for useful discussions. This work is supported by AFOSR Grant AF-F49620-01-1-0331. LBNL

TEM work was supported by AFOSR (Order No. OGMORD52K44149), through the U.S. Department of Energy under Contract No. DE-AC03-76SF0098. J. B. J. and Z. L.-W. would like to acknowledge the use of the facilities at the National Center for Electron Microscopy at LBNL.

Footnotes and References

a) Electronic mail: ycao@nd.edu

b) Electronic mail: dhall@nd.edu

¹ T. Mimura and M. Fukuta, IEEE Trans. Electron Devices **27**, 1147 (1980).

² C. W. Wilmsen, (Plenum, New York, 1985).

³ M. Passlack, J. K. Abrokwhah, R. Droopad, Z. Y. Yu, C. Overgaard, S. I. Yi, M. Hale, J. Sexton, and A. C. Kummel, IEEE Electron Device Letters **23**, 508 (2002).

⁴ P. D. Ye, G. D. Wilk, B. Yang, J. Kwo, S. N. G. Chu, S. Nakahara, H. J. L. Gossmann, J. P. Mannaerts, M. Hong, K. K. Ng, and J. Bude, Appl. Phys. Lett. **83**, 180 (2003).

⁵ P. D. Ye, G. D. Wilk, B. Yang, J. Kwo, H. J. L. Gossmann, M. Hong, K. K. Ng, and J. Bude, Appl. Phys. Lett. **84**, 434 (2004).

⁶ M. Passlack, N. Medendorp, S. Zollner, R. Gregory, and D. Braddock, Appl. Phys. Lett. **84**, 2521 (2004).

⁷ J. M. Dallesasse, N. Holonyak, Jr., A. R. Sugg, T. A. Richard, and N. El-Zein, Appl. Phys. Lett. **57**, 2844 (1990).

⁸ P. Parikh, Ph. D. Thesis, U. California at Santa Barbara, 1998.

- ⁹ S. S. Shi, E. L. Hu, J. P. Zhang, Y. I. Chang, P. Parikh, and U. Mishra, *Appl. Phys. Lett.* **70**, 1293 (1997).
- ¹⁰ M. R. Islam, R. D. Dupuis, A. P. Curtis, and G. E. Stillman, *Appl. Phys. Lett.* **69**, 946 (1996).
- ¹¹ C. I. H. Ashby, J. P. Sullivan, P. P. Newcomer, N. A. Missert, H. Q. Hou, B. E. Hammons, M. J. Hafich, and A. G. Baca, *Appl. Phys. Lett.* **70**, 2443 (1997).
- ¹² A. L. Holmes, Ph. D. Thesis, U. of Texas at Austin, 1999.
- ¹³ P. J. Barrios, D. C. Hall, G. L. Snider, T. H. Kosel, U. Chowdhury, and R. D. Dupuis, in *State-of-the-Art Program on Compound Semiconductors (SOTAPOCS XXXIV), Electrochemical Society Proceedings* (2001), Vol. 2001-1, pp. 258.
- ¹⁴ X. Li, Y. Cao, D. C. Hall, P. Fay, X. Zhang, and R. D. Dupuis, *J. Appl. Phys.* **95**, 4209 (2004).
- ¹⁵ P. Y. Yu and M. Cardona, in Fundamentals of Semiconductors: Physics and Materials Properties (Springer, Berlin, NY, 2001), pp. 566.
- ¹⁶ Y. Cao, J. Zhang, X. Li, T. H. Kosel, P. Fay, P. Barrios, D. C. Hall, R. E. Cook, X. Zhang, and R. D. Dupuis, presented at the 46th Electronic Materials Conference, Notre Dame, Indiana, 2004 (unpublished).
- ¹⁷ M. J. Graham, S. Moisa, G. I. Sproule, X. Wu, J. W. Fraser, P. J. Barrios, D. Landheer, A. J. SpringThorpe, and M. Extavour, *Mater. High Temp.* **20**, 277 (2003).
- ¹⁸ M. Passlack, M. Hong, J. P. Mannaerts, R. L. Opila, S. N. G. Chu, N. Moriya, F. Ren, and J. R. Kwo, *IEEE Trans. Electron Devices* **44**, 214 (1997).
- ¹⁹ L. G. Meiners, *J. Vac. Sci. Technol.* **15**, 1402 (1978).
- ²⁰ J. Y. Wu, P. W. Sze, Y. H. Wang, and M. P. Houn, *Solid-State Electron.* **45**, 1999 (2001).
- ²¹ P. J. Barrios, S. K. Cheong, D. C. Hall, N. C. Crain, G. L. Snider, C. B. DeMelo, T. Shibata, B. A.

Bunker, U. Chowdhury, R. D. Dupuis, G. Kramer, and N. El-Zein, presented at the 42nd Electronic Materials Conference, Denver, Colorado, 2000 (unpublished).

²² J. Y. Wu, H. H. Wang, Y. H. Wang, and M. P. Houg, IEEE Electron Device Letters **20**, 18 (1999).

Tables

TABLE I. Comparison of the leakage current densities, J_L , at applied field of 1 MV/cm (except as noted) and breakdown fields, E_B , for various deposited and native oxide insulators and thicknesses, d , on GaAs. All devices are MOS capacitors except as noted.

Insulator	d (nm)	J_L (A/cm ²)	E_B (MV/cm)	Ref.
Ga ₂ O ₃ (As ₂ O ₃) ^a	30	1.2x10 ⁻⁴	5.3	20
Gd _{0.31} Ga _{0.1} O _{0.59} / Ga ₂ O ₃	64	1x10 ⁻⁹	3.5	6
Al ₂ O ₃	8	9x10 ⁻⁸	5	4
InAlP oxide	110	9x10 ⁻¹¹ ^b	6.3	13
Al ₂ O ₃ ^a	16	<10 ⁻⁴ ^c	N. R.	5
AlGaAs oxide	45	4.9x10 ⁻⁷	3.8	21
Ga ₂ O ₃ (As ₂ O ₃)	65	2x10 ⁻⁷	4.7	22
InAlP oxide	48	8.7x10 ⁻¹¹	3-6	This work
InAlP oxide	17	1.4x10 ⁻⁹	3-6	This work

^aMOSFET

^b Maximum measurement voltage of 5 V (0.45 MV/cm)

^c Range reported for voltages < 3V (<1.88 MV/cm)

N. R. = not reported

Figure Captions

FIG. 1. Typical current density versus electric field curves for MOS capacitors with (a) 17 nm and (b) 48 nm thick InAlP native oxide films on *n*-type GaAs substrates. The capacitor contact area $A=5.8 \times 10^{-4} \text{ cm}^2$. Sweep rate is 10 mV/s.

FIG. 2. Comparison of bright field TEM images of (a) 110 nm and (b) 17 nm thick InAlP wet thermal native oxide films. The particles clearly visible in (a) are not present anywhere in sample (b).

FIG. 3. High-frequency (CH, 100 kHz) and quasi-static (CQ) capacitance-voltage measurements for 17 nm native oxide of InAlP on (a) *n*-type and (b) *p*-type GaAs. Sweep rate is 50 mV/s. CQ data show inversion for both carrier types, indicating an unpinned Fermi level.

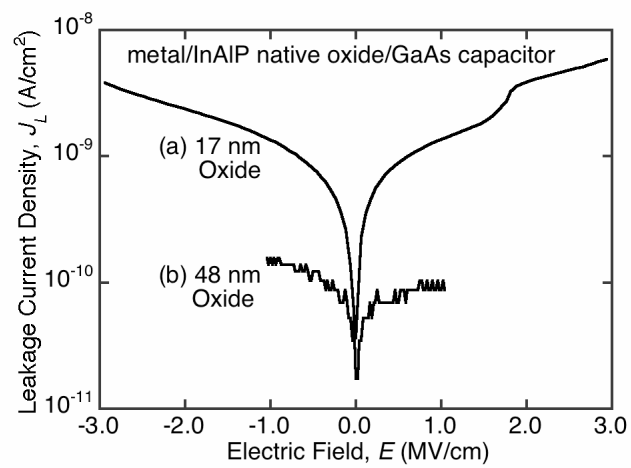


Fig. 1 Y. Cao et al.

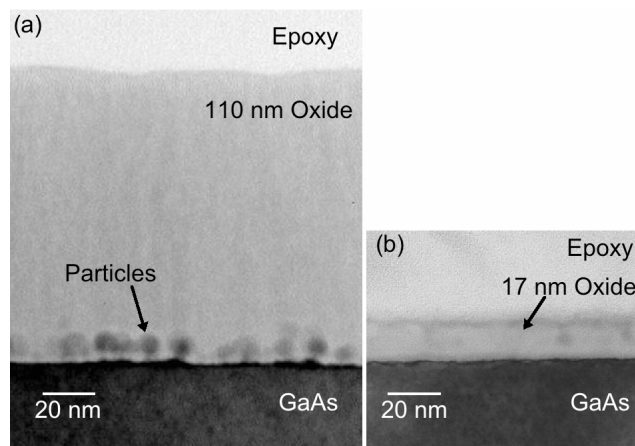


Fig. 2 Y. Cao et al.

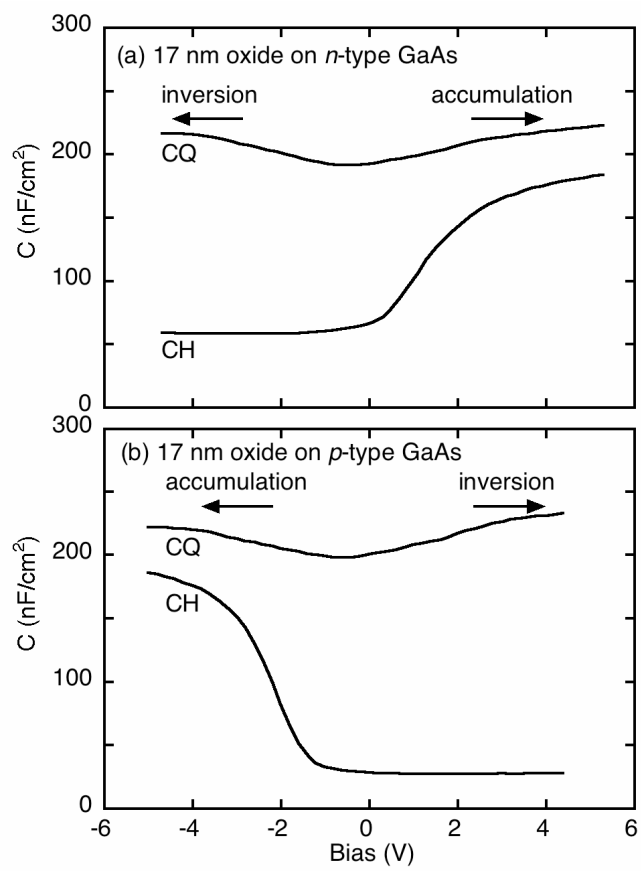


Fig. 3 Y. Cao et al.